UNIVERSITY OF HELSINKI

https://helda.helsinki.fi

New column simulations for the Viking landers : Winds, fog, frost, adsorption?

Savijärvi, Hannu; Paton, Mark; Harri, Ari-Matti

2018-08
Academic Press Inc.
http://hdl.handle.net/10138/314708
Savijärvi, H, Paton, M & Harri, A-M 2018, 'New column simulations for the Viking landers : Winds, fog, frost, adsorption?', Icarus, vol. 310, pp. 48-53. https://doi.org/10.1016/j.icarus.2017.11.007

Downloaded from Helda, University of Helsinki institutional repository. https://helda.helsinki.fi
This is an electronic reprint of the original article.
This reprint may differ from the original in pagination and typographic detail.
Please cite the original version.

New column simulations for the Viking landers: winds, fog, frost, adsorption?

Hannu Savijärvi[1,2,*], Mark Paton[2], Ari-Matti Harri[2]

[1]Department of Physics, University of Helsinki, 00140 Helsinki, Finland
[2]Finnish Meteorological Institute, Helsinki, Finland

Abstract

Boundary layer simulations are shown for the first sols of the two Viking landers on Mars. The column model (with cloud/radiation interaction and Prandtl slope wind terms) used successfully for winds, fogs and clouds at Phoenix is equipped here with an adsorption-diffusion scheme for water vapor transport in porous regolith. The model's 1.6 m temperatures and winds are quite close to those observed by the two landers; in particular the weak summer slope winds of VL-2 are excellently reproduced.

The model predicts for both sites diffusion and adsorption of water into regolith in the evening, thin ground frost deposition from about midnight, and an early morning fog with an inflection in T1.6m slightly weaker than observed. At the moister VL-2 site fog increases optical depth as observed. Fogs and frosts sublimate away after sunrise, allowing desorption and diffusion of water off the sun-heated regolith. For porosity of 22% PWC is approximately conserved from sol to sol with only little diurnal variation, as the depleted layer of air moisture is quite shallow.

In simulations without adsorption frost forms early and it grows thick. At VL-2 fog now forms too early and the jump in optical depth is larger than observed. At the drier VL-1 fog still forms nearly as with adsorption, so observations could also be explained without adsorption. On the other hand VL-1 certainly landed onto porous regolith and heavy frost was not observed. Hence it is suggested that adsorption is likely at both VL sites in summer.

Keywords: Mars, climate Mars, surface Meteorology

[*]Corresponding author at: Department of Physics, 00014 University of Helsinki, Finland
E-mail address: hannu.savijarvi@helsinki.fi
Tel: +358-40-9380858

1. Introduction

The Viking 1 and Viking 2 landers (VL-1, VL-2) landed onto Mars in 1976 during local summer at about 22.5ºN, 48.0ºW, Ls 97º and 48.0ºN, 225.7ºW, Ls 117º, respectively. Their first-ever weather observations from the surface of Mars are reported in Pollack et al. (1977; optical depth) and Hess et al. (1977; surface pressure, air temperature and wind together with surface temperatures from the Viking orbiters). The Mars Atmospheric Water Detector (MAWD) onboard the orbiters charted column moisture (Farmer et al., 1977). Many landers and rovers have since provided surface data from Mars, including observations of relative humidity (RH) and water vapor mixing ratio (q) for more than two Mars years from the Rover Environmental Measuring Station humidity device (REMS-H) of the Mars Scientific Laboratory (MSL) onboard the Curiosity rover in the Gale crater (Gomez-Elvira et al., 2014, Harri et al., 2014). All the in-situ meteorology observations from Mars up to 2016 are described and reviewed in Martinez et al. (2017).

The Viking and other lander data have provided validation for various atmospheric models, from local column models to GCMs. Here the University of Helsinki/Finnish Meteorological Institute 1-D column model is applied at the VL sites (since Savijärvi, 1991; 1995). The aim is to validate the 2017 model version with its radiatively active clouds, slope winds and adsorptive regolith, and in particular, to discuss the summertime diurnal cycle of near-surface moisture at the VL sites in the light of the simulations and available indirect indications of moisture. Jakosky et al. (1997, J97) suggested that some processes (possibly frost or adsorption to porous regolith) depleted water vapor every night at both sites, while Pollack et al. (1977) suggested that the early morning increases in optical depths could be due to fog. Frost persisted throughout the day at VL-2 in wintertime (Martinez et al., 1977).

The REMS-H observations strongly suggest adsorption to take place at Gale. The UH/FMI 1-D model with a diffusion-adsorption scheme could closely simulate the daily cycles of RH and q at Curiosity (Savijärvi et al., 2016), whereas without adsorption it could not (Savijärvi et al., 2015). Steele et al. (2017) came to the same conclusion in mesoscale model experiments for Gale. Zent et al. (2016) found both adsorption and frost from recalibrated TECP data at polar Phoenix. Frosts and fogs appear nonexistent at equatorial Curiosity (Martinez et al., 2016, 2017), but they could occur at subtropical VL-1 and high-latitude VL-2. Transient midnight formation of salty brines could also occasionally deplete some air moisture at Curiosity (Martin-Torres et al., 2015) but this effect is probably small and is not included in the present VL experiments.

Water vapor diffusion and adsorption into porous soil is sensitive to the surface flux of moisture (Savijärvi et al., 2016, Steele et al., 2017), whereas frost cuts the flux off and fog may reduce it. Frosts, fogs and fluxes are all notoriously sensitive to winds, temperatures and local stabilities, so a realistic simulation of the diurnal cycle of moisture needs first of all to have the near-surface winds and temperatures about right. This is another reason for our return to the Vikings, as winds from their first sols, when all instruments were working properly, are still probably the best available for model validation. Moreover, as will be seen, the two VL sites provide nearly ideal environments for column models, especially during the mild northern midsummer when the VL's arrived to Mars.

2. The column model

Only a brief account is given here; the references below provide details. The UH/FMI 1-D model is a hydrostatic boundary layer column model without advections. It is driven by a given large-scale geostrophic wind $\mathbf{V}_g$ and the varying surface temperature, which is predicted from the surface heat budget. The model's dynamics includes here a simple Prandtl theory –based slope wind mechanism. Turbulence is via a mixing length theory with a Monin-Obukhov surface layer, the vertical turbulent

fluxes (including the moisture flux) depending on local stability and wind speed. The slope wind terms, stability functions and cloud physics are the same as described in Savijärvi and Määttänen (2010) for Phoenix, where the model simulated the "telltale"-observed winds and the LIDAR-observed night fogs and boundary layer clouds rather well.

The moisture predictands are the mass mixing ratio of water vapor (q) and water ice (q_i), ice condensing onto dust particles. Radiation (CO_2, water vapor, dust, fogs and iceclouds being active) is based on a broadband LW emissivity scheme and an improved delta-two-stream broadband SW scheme, both validated against line-by-line results in Savijärvi et al. (2005). Ice may also condense at the surface (ground frost) as well as within the pores of the regolith. The eight-layer regolith scheme includes vertical diffusion of soil temperature and pore volume moisture together with the strongly temperature-dependent adsorption of moisture onto regolith grains. The regolith scheme is as described in Savijärvi et al. (2016) for MSL, where it gave a good simulation when using the palagonite-based adsorption isotherm of J97, which is also adopted here. If porosity is set to 0 (as for rocky ground), there is no adsorption and no moisture exchange through the surface.

The present Prandtl version is rather similar in its dynamics to the dry boundary layer model of Haberle et al. (1993). They also made comparisons with VL data, to be commented later. In our model the atmospheric column contains 29 grid points, the lowest being at 0, 0.3, 0.7, 1.6, 3.7, 8.5 m … from the surface; the top is at 50 km. Time step is 10 s. Initially (0000 local solar time, LT) winds are set to $\mathbf{V}_g$, and T to 220K at the surface with lapse of 1.5K/km. $\mathbf{V}_g$ and q(z) are broadly based (in lack of observations) on the VL site values of the GCM-derived Mars Climate Database (MCD). The results are shown from the third sol, when the model is repeating its diurnal cycle. The basic simulations are made with adsorption active; alternatively the surface interactions of moisture are shortcut by setting porosity of the soil to 0.

3. Validation of the model: summer temperatures and winds at the VL sites

For the first-sols simulations of VL-1 at 22.5°N, L_s is set to 100° and the main atmospheric and site parameters (surface pressure 765 Pa, surface albedo 0.22, thermal inertia 283 SI units, roughness length 1 cm, dust optical depth 0.5) are based on observations and literature. A thin aphelion high cloud with optical depth of 0.07 is also present, as indicated by multiannual orbit observations (e.g. Smith, 2004). Upslope of 0.10° points to 247° (WSW); this provides the best match with the observed winds (obtained in Haberle et al. (1993) with 0.17° slope to SW).

Figure 1 shows the resulting model temperature profiles from 1.6 m to 5 km at 0600, 1000, 1600 and 2200LT. At 1.6 m the temperatures are within ± 2K to the observed values for the first VL-1 sols from Hess et al. (1977); these were quite repetitive from sol to sol. Also shown in Figure 1 are two measured temperatures during the parachute landing of VL-1 at about 1615LT (Seiff and Kirk, 1977). The model's 1600LT T-profile is close to the observations, displaying a convective nearly adiabatic profile up to 4 km. After the development of a nocturnal strongly stable radiative surface inversion (to about 1 km height by 0600LT) the convective layer grows again in the morning, extending to about 700 m by 1000LT with a strongly superadiabatic layer near the surface in Figure 1. The physics of the boundary layer temperature evolution is discussed in more detail in Petrosyan et al. (2011) and in Savijärvi (2012a, 2012b).

Figure 2 displays the diurnal air and frost point temperatures at 1.6 m (T, T_f) and the ground surface temperature (T_g) from the VL-1 simulations with and without adsorption. T and T_g are the same in the two simulations, T ranging between 188-241K and T_g between 185-263K, as reported for the first VL-1 sols (Hess et al., 1977). T_g exceeds T from about 0730LT, triggering convection, and falls below T at around 1645LT, the surface layer then turning from convective to stable. The frost point

temperatures are discussed later.

Observed VL-1 winds at 1.6 m varied from sol to sol, although following a quite repetitive diurnal pattern. Hence Figure 3 displays the sol 0-44 mean diurnal wind hodograph from Hess et al. (1977), together with model 1.6 m winds for a) no prevailing geostrophic wind (V_g 0, open squares), and b) constant $\mathbf{V}_g$ of 10 m/s from 180^o (black triangles). Observed winds are down the slope during the night, then strengthen and turn anticlockwise to upslope winds during the convective hours, weakening and turning clockwise again in the evening and night. The V_g 10 m/s simulation produces about the same, although the match is not perfect. In contrast, the V_g 0 simulation displays pure low-latitude slope winds, which turn clockwise by the weak Coriolis force all the time. On the other hand, without any slope the model's 1.6 m winds for V_g 10 m/s from S (not shown) are about 5 m/s from 160^o during daytime, and about 2 m/s from 130^o during the night. Thus our simple 1-D Prandtl model appears to confirm the broadly similar 2-D slope model results of Savijärvi and Siili (1993): during vigorously convective daytime the large-scale wind is mixed down to the surface, where it adds to and interacts with the local slope winds. This leads to stronger speeds and anticlockwise rotation, whereas during the stable evening and night vertical mixing is weak and slope winds may hence dominate near the surface. Curiously, Haberle et al. (1993) could simulate the anticlockwise turning in their 1-D model without any stated geostrophic wind.

Seiff (1993) inferred winds from VL-1 parachute movements at 1.5-3.5 km, obtaining about 20 m/s from the SE quadrant. Our V_g 10 m/s simulation, Haberle et al. (1993), and MCD do also indicate winds from SE for these heights but with weaker speeds, 2-7 m/s. The free-atmosphere MCD winds (~$\mathbf{V}_g$) are also from the S-SE sector, being 8-10 m/s during late morning but weakening toward the night. Weak nocturnal large-scale winds might explain why in Figure 3 the model winds for no V_g are actually closer to the observed winds during the night than with V_g of constant 10 m/s.

In the VL-2 first-sol simulations latitude is 48^{o}N, L_s 120^o, surface pressure 770 Pa, albedo 0.2, thermal inertia 350 SI units, roughness length 1 cm, dust optical depth 0.3, and upslope of 0.1^o is to the east (90^o). The model's T1.6 m (Figure 4) then ranges between 192-241K and T_g between 191-263K, as was observed for the first VL-2 sols (Hess et al., 1977). An excellent match with the observed mean winds (Figure 5) is here obtained without any large-scale wind (MCD winds being weak, < 5 m/s below 10 km). Figure 5 displays a pure high-latitude strong-Coriolis-force slope wind cycle, with upslope winds at midday, downslope winds at night and rapid continuous clockwise turning. However, during the sensitive afternoon stabilization period the observed winds appear more variable than in the model. The Haberle et al. (1993) single-column simulation for VL-2 winds with no V_g was also quite good; their best-match winds resulted from upslope of 0.1^o set to the northeast.

These good results suggest that the column models are doing a good job, but also that conditions are rather favorable for them at the VL sites. In particular the gently sloping plane around the VL-2 site is very homogeneous, smooth and flat (this is the main assumption of the Prandtl slope wind theory). Furthermore, the prevailing flow is weak in summertime, especially at VL-2, so that local advections and other 3-D effects (which are not included in the 1-D models) are minimal and thus slope effects may dominate the surface winds.

4. VL-2 moisture results and discussion

We now turn to the moisture results, starting from VL-2. The near-surface midsummer air is relatively moist at the high-latitude VL-2 site since the north pole water ice cap has just sublimated completely. The column precipitable water content (PWC) was charted by MAWD onboard the Viking orbiters. The vertical structure was, however, not constrained. Hence the initial q(z) is

adopted from MCD at the landing season (PWC 33-34 μm), but scaled to produce the actual MAWD-observed PWC above the VL-2 site, about 25 μm at Ls 120-130^o (J97, their fig. 2). Figure 6 shows the resulting initial profile and diurnal profiles of q from sol 3 in the VL-2 simulation with adsorption. One may note a well-mixed layer of q ~200 ppmm to about 4 km height in Figure 6 and strong depletion of q very near the surface (by adsorption) during the evening and night. At 0600LT an increase in q can be seen just above the sun-warmed surface (sunrise occurred here at 0425LT). This very shallow convective layer grows to about 750 m by 1000LT. PWC stays at around 25 μm from sol to sol in the VL-2 simulation, as observed, provided the porosity of the soil is set to 22%.

Figure 7 displays the mixing ratios of water vapor and water ice at 1.6 m (q, q_i, in ppmm) and the frost depth at the ground (in 0.01 μm).
The adsorption case is discussed first. The values of T1.6m and T_g (Figure 4) are to within $\pm$ 2K to those shown in Hess et al. (1977) and are practically the same in the two simulations. Convection starts at about 0530LT when T_g exceeds T; stabilization ($T_g < T$) respectively at about 1800LT. The afternoon values of q are near 200 ppmm in both simulations (Figure 7). In the adsorption case (thick line) adsorption of water vapor to the rapidly cooling regolith increases strongly after 1800LT, thus reducing q. Hence the air frost point (T_f, thick dots in Figure 4) decreases in the evening. It meets T_g at 0000LT, whence frost begins to deposit onto the cold ground. The frost depth (thick dashed line in Figure 7) grows to 0.18 μm by 0500LT and disappears by 0700LT. Fog (q_i at 1.6 m; thick dotted line in Figure 7) appears between 0100-0200LT, q_i reaching 111 ppmm by 0600LT with precipitable ice content of 0.32 μm then across the about 100 m high fog layer, and disappears by 0800LT. The optical depth increases in the model accordingly from 0.3 at daytime (dust only) to 0.42 by 0600LT (dust plus fog with ice particle effective radius of 5 μm assumed), as typically observed at VL-2 by imaging the sun about one hour before and after sunrise during Ls 120-130^o (Pollack et al., 1977; their fig. 2).

The relatively high midsummer night T_g and the strong evening depletion of water vapor by adsorption (Figures 4, 6, 7) keep the deposited frost amount low, despite high values of moisture of the early afternoon. The latter are partly due to desorption of water from the rapidly warming regolith at 0700-1300LT, after frost has sublimated away by 0700LT. As enthalpy of sublimation (46.7 kJ/mol) is higher compared to that of adsorption of water (about 23 kJ/mol according to REMS data, Savijärvi et al., 2015, 2016), the q-slopes are accordingly much steeper in Figure 7 during the deposition (0100-0500LT) and sublimation (0500-0700LT) of frost than during the periods of adsorption (1800-0100LT) and desorption (0700-1300LT).

In the VL-2 no porosity simulations (thin lines in Figures 4,7) q stays high until about 2100LT, when T_g hits T_f and relatively strong formation of ground frost begins to rapidly deplete air moisture. Thick fog now appears just after midnight and reaches 161 ppmm at 1.6 m by 0700LT with optical depth jumping to 0.53 before being dissolved by the increasing morning sunshine. The frost depth grows to 0.9 μm by 0500LT; its subsequent rapid sublimation makes the 0800LT peak to the near-surface air humidity q. Nearly the same results are obtained by setting adsorption to 0 but allowing the (then non-scaled) molecular/Knudsen diffusion of water vapor in porous regolith (see Savijärvi et al., 2016). Hence diffusion as such (i.e., without adsorption) appears to be ineffective in the diurnal-scale water exchange between the atmosphere and top regolith.

Frost has not been observed so far by MSL in the dry Gale crater at 4^{o}S, but in the mesoscale Gale simulations of Steele et al. (2017) frosts appear in the surrounding regions. During the moist season (Ls 180^o) they amount to depths of ~0.2-0.3 μm with adsorption and up to 0.8 μm without adsorption; rather similarly with the above VL-2 results.

Ryan and Sharman (1981, their Table 1) report for the first sols of VL-2 a composite 1.6 m

temperature inflection at around 0130LT, with fog formation suggested as the reason. Our adsorption simulation agrees nicely with this, but the two no-adsorption simulations induce fog too early (0000LT vs. 0130LT) and the nocturnal increase in optical depth is too large in them (0.23 vs. observed 0.1-0.15). Furthermore, the inflection-based estimate for PWC is 10.5-12 μm for VL-2 at around L_s 120° in J97 (their fig. 2). A similar estimate from the adsorption simulation (i.e. having the 0130LT q at 1.6 m vertically constant in the integration for PWC) produces 11 μm, but from the no-adsorption simulations, 15 μm. It thus appears that adsorption is very likely at the VL-2 site in summer.

We made some sensitivity tests about the robustness of the assumed values of PWC and porosity. Fedorova et al. (2010) have suggested lower values for retrieved PWC from MAWD, by about 40% for VL-2 latitude means at around Ls 120°. Hence the VL-2 simulation was repeated with initial PWC scaled to 15 μm. Here fog appeared between 0300-0400LT, i.e. too late; and there was no increase in optical depth, the fog remaining too thin for that. As MCD (~34 μm) and later retrievals of PWC at 48°N, 120° Ls (by TES and CRISM, for MY26-34) appear to be rather in the 22-35 μm range, we believe that the VL-2 results with PWC of 25 μm are the more relevant.

The porosity of 22% was assumed here, because it conserved PWC from sol to sol in the VL-2 simulation (as was observed in J97). With PWC initially 25 μm, porosity of 40% led to a slow daily increase of PWC (to 27.5 μm by sol 4) and to a morning fog, which was increasingly too early and too thick. Porosity of 10% produced on the other hand slow reduction in PWC (to 24.2 μm by sol 4) and a fog, which was increasingly late and too thin. Admittedly, this result (as all others) might depend heavily on the adsorption scheme chosen; we used the J97 adsorption isotherm, which appeared to be the best in the MSL REMS data vs. model comparisons of Savijärvi et al. (2016) and Steele et al. (2017).

5. VL-1 moisture results and discussion

At the VL-1 site around Ls 100-110° the MAWD-observed PWC is about 12.5 μm (J97, their fig. 1) and MCD-PWC is 12-14 μm with maximum of q at about 10 km height, indicating the water pulse transported to the south from the sublimating northern icecap (Read and Lewis, 2004; Smith, 2004). Figure 8 displays the initial and diurnal sol 3 q-profiles from the VL-1 simulation with adsorption. Strong convection mixes the water vapor evenly to about 65 ppmm in the lowest 4 km during daytime. The vapor then stays well-mixed over the night except close to the surface, where it is strongly depleted in a shallow layer during the evening and night. The depleted moisture returns to the growing convective layer next morning (note the 1000LT curve) and hence PWC stays at around 12.5 μm from sol to sol in the integration (as observed), provided porosity is set to 22% at the VL-1 site as at VL-2 (35-40% was suggested for the MSL landing site and Rocknest in Savijärvi et al., 2016). There is only little diurnal variation in PWC because the depleted layer is so shallow.

Ryan and Sharman (1981) report inflections in the observed VL-1 temperatures during many nights, typically at 0200-0300LT, followed by slightly enhanced atmospheric opacities (Pollack et al. 1977). The inflection was suggested to be due to the radiative effect of a developing fog. The nighttime increase in opacity was smaller than at VL-2 and nonexistent at Ls 105-110°, so the fog was probably much weaker than at VL-2.

We discuss first the simulation with adsorption. Its T_f (thick dotted line) hits T_g after 2300LT in Figure 2 (weak frost then starting to form onto the cold ground), and T between 0200-0300LT (fog forming at 1.6 m) with a trace of an inflection in T, although the inflection is weaker than in the observations. Figure 9 displays the diurnal moisture evolution at and near the surface in the VL-1

case. In the adsorption simulation (thick lines) q begins to decay rapidly after 1700LT because adsorption is activated by the rapid decrease of T_g (Figure 2). This depletes humidity from the near-surface air; replenishment from the moister layers aloft (Figure 8) is inhibited by the weak turbulent mixing of the now very stable surface layer. From 2400LT onward frost (thick dashed line) is seen to deposit on the ground. It replaces adsorption as the moisture-depleting process. The very thin frost layer grows to about 0.15 μm by sunrise. From 0200-0300LT also icefog appears at 1.6 m (thick dotted line), in accordance with the Ryan and Sharman suggestion. Fog grows to about 20 m height by 0600LT with q_i about 7 ppmm throughout, but its precipitable ice content is only 0.006 μm. This is too little to cause strong radiative warming though the optical depth of the atmosphere is slightly enhanced (from 0.5 (dust) to 0.52). Soon after sunrise (0530LT) the thin fog and frost sublimate back to vapor; then upward diffusion and desorption from the rapidly warming regolith releases more vapor, which mixes evenly to the growing convective boundary layer, as seen in Figure 8.

In the no-adsorption simulation q (thin line in Figure 9) stays nearly constant during the afternoon and evening until at about 2200LT the associated higher T_f (thin dotted line in Figure 2) hits T_g and frost begins to strongly deposit onto the cold ground. Hence q and T_f decrease and at about 0230 fog (thin dotted line in Figure 5) does appear much as in the basic simulation. Frost (thin dashed line in Figure 5) grows here up to 0.4 μm by 0700LT but sublimates rapidly back to vapor by 0800LT, increasing q temporarily at 0800LT. (Such a peak in moisture was noted at Phoenix after frosty nights (Zent et al., 2016), and in the no-adsorption (hence frosty) Gale simulations of Steele et al. (2017)). After the morning peak q stays here nearly constant late to the evening.

Because the fog and the temperatures are nearly the same in the VL-1 simulations with and without adsorption, the VL-1 fog-related observations do not ascertain adsorption. On the other hand VL-1 is known to have landed onto loose material: the three legs of the lander were buried several cm deep into it. The temperature sensor for the parachute landing (Figure 1) was fixed to one of the legs. Fortunately it survived the landing and made a long within-soil temperature record, from which some of the properties (e.g. the particle diameter of 8 μm) of the fine-grained porous regolith could be estimated (Paton et al., 2016). Moreover, summer frosts are not reported for VL-1 (Martinez et al., 2017). Hence adsorption to porous regolith is likely to take place also at the VL-1 site.

The sensitivity tests for PWC and porosity gave results similar to those at VL-2: with 40% reduced initial PWC (7.5 μm) no fog formed at VL-1. With PWC of 12.5 μm and porosity of 44% (10%) the night fog was getting stronger and earlier (weaker and later) with PWC increasing (decreasing) unrealistically from sol to sol. Thus porosity of 22% is tentatively suggested for both VL sites.

6. Conclusion

We simulated the first sols of VL-1 and VL-2 on Mars using a column model with adsorption, and compared with observations from literature. Orbit-observed ground temperatures and diurnal 1.6 m air temperatures were well simulated at both sites. The VL-2 mean diurnal winds were very well reproduced without any V_g, suggesting that the midsummer large-scale winds are weak at this site. Hence the near-surface winds are purely slope-driven. The main features of the more complex VL-1 winds were reproduced by having a suitable basic flow (constant V_g of 10 m/s from south representing the seasonal western boundary current of the site) interacting with the diurnal slope winds. These 1-D model results and conclusions are compatible with the 2-D simulations of Savijärvi and Siili (1993).

The VL-2 model with its good near-surface temperature and wind simulation provides hope for a

realistic moisture simulation. The initial mixing ratio profile was adopted from MCD and scaled to produce the MAWD-observed actual PWC of about 25 μm. Moisture was then evenly mixed in the lowest 4 km every afternoon (~200 ppmm) by vigorous convection. During the evening downward diffusion and adsorption to porous regolith, and from midnight onward weak frost deposition, depleted moisture from the stable near-surface air. After sunrise sublimation, desorption, upward diffusion and convection returned the moisture back to the growing well-mixed layer. With the tentatively suggested porosity of 22% PWC was conserved from sol to sol at 25 μm with only little diurnal variation, since the depleted layer of air moisture was quite shallow.

Air moisture was unfortunately not directly observed by the Viking landers. However, at VL-2 an inflection in T1.6m was typically observed at about 0130LT, followed by an increase of about 0.1 in optical depth, both suggesting a thin radiation fog. The model with adsorption did develop an icefog with a weak inflection in T1.6m and an increase of optical depth very nearly as was observed. In contrast, simulations without adsorption produced heavy frost, with fog and the related T-inflection occurring too early and the increase in optical depth being too large compared to the observations. Thus adsorption is very likely at VL-2.

The drier VL-1 simulation with adsorption is also consistent with observations: having PWC as by MAWD (12.5 μm) the observed inflection in T1.6m occurs (again via formation of a very thin fog) at about the correct time and temperature. However, here the no-adsorption simulation, due to heavy frost strongly depleting air moisture, leads to practically the same 1.6 m values of q, T and fog as did the simulation with adsorption, so the VL-1 observations could also be explained without adsorption. Hence adsorption is not certain at VL-1. Still, we suggest that adsorption is likely also at VL-1, because it is known that VL-1 landed onto porous regolith, and frost has not been reported at VL-1 during the summer.

Acknowledgements:

References:

Farmer CB, Davies DW, Holland AL, LaPorte DD, Doms PE, 1977. Mars: Water vapor observations from the Viking Orbiters. J. Geophys. Res. 82, 4225-4248.

Gómez-Elvira GJ et al., 2012. REMS: The Environmental Sensor Suite for the Mars Science Laboratory Rover. Space Sci. Rev. 170, 583-640, doi:10.1007/s11214-012-9921-1.

Haberle RM, Houben HC, Hertenstein R, Herdtle T, 1993. A boundary-layer model for Mars: Comparison with Viking Lander and entry data. J. Atmos. Sci. 50, 1544-1559.

Harri AM et al., 2014. Mars Science Laboratory relative humidity observations: Initial results. J. Geoph. Res. Planets 119, 2132-2147, doi: 10.1002/2013JE004514

Hess SL, Henry RM, Leovy CB, Ryan JA, Tillman JE, 1977. Meteorological results from the surface of Mars: Viking 1 and 2. J. Geophys. Res. 82, 4559-4574.

Jakosky BM, Zent AP, Zurek RW, 1997. The Mars water cycle: Determining the role of exchange with the regolith. Icarus 130, 87-95.

Martínez GM, Fischer E, Rennó NO, Sebastián E, Kemppinen O, Bridges N, Borlina CS, Meslin PY, Genzer M, Harri AM, Vicente-Retortillo A, 2016. Likely frost events at Gale crater: analysis from MSL/REMS measurements. Icarus 280, 93–102.

Martínez GM, Newman CN, De Vicente-Retortillo A, Fischer E, Renno NO, Richardson MI, Fairén AG, Genzer M, Guzewich SD, Haberle RM, Harri AM, 2017. The Modern Near-Surface Martian Climate: A Review of In-situ Meteorological Data from Viking to Curiosity. Space Sci. Rev. pp.1-44.

Martin-Torres et al., 2015. Transient liquid water and water activity at Gale crater on Mars. Nature Geoscience, doi:10.1038/NGEO2412

Paton MD, Harri A-M, Mäkinen T, Savijärvi H, Hagermann A, Kemppinen O, Johnston A, 2016. Thermal and microstructural properties of fine-grained material at the Viking Lander 1 site. Icarus 271, 360-374. doi:10.1016/j.icarus.2016.02.012.

Petrosyan A, Galperin B, Larsen SE, Lewis SR, Määttänen A, Read PL, Renno N, Rogberg LPHT, Savijärvi H, Siili T, Spiga A, Toigo A, Vazquez L, 2011. The Martian atmospheric boundary layer. Reviews of Geophysics 49, RG3005, doi: 10.1029/2010RG000351

Pollack JB, Colburn D, Kahn R, Hunter J, Van Camp W, Carlston CE, Wolf MR, 1977. Properties of aerosols in the martian atmosphere, as inferred from Viking Lander imaging data. J. Geophys. Res. 82, 4479-4496.

Read PL, Lewis SR, 2004. The Martian Climate Revisited. Springer-Praxis, UK, 325 pp.

Ryan JA, Sharman RD, 1981. H2O frost point detection on Mars? J. Geophys. Res. 86 C1, 503-511.

Savijärvi H, 1991. A model study of the PBL structure on Mars and the Earth. Contr.Atmos.Phys., 64, 219-228.

Savijärvi H, Siili T, 1993. The Martian slope winds and the nocturnal PBL jet. J. Atmos. Sci. 50, 77-88.

Savijärvi H, 1995. Mars boundary layer modeling: Diurnal moisture cycle and soil properties at the Viking Lander 1 site. Icarus, 117, 120-127.

Savijärvi H, Crisp D, Harri AM, 2005. Effects of CO2 and dust on present-day solar radiation and climate in Mars. Quart.J.Roy.Meteor.Soc., 131, 2907-2922.

Savijärvi H, Määttänen A, 2010. Boundary-layer simulations for the Mars Phoenix lander site. Quart. J. Roy. Meteor. Soc., 136, 1497-1505, doi:10.1002/qj.650

Savijärvi H, 2012a. Mechanisms of the diurnal cycle in the atmospheric boundary layer of Mars. Quart. J. Roy. Meteor. Soc. 138, 552-560. doi:10.1002/qj.930

Savijärvi H, 2012b: The convective boundary layer on Mars: some 1-D simulation results. Icarus 221, 617-623.

Savijärvi H, Harri AM, Kemppinen O, 2015. Mars Science Laboratory diurnal moisture observations and column integrations. J.Geophys.Res. Planets, 120, 1011-1021, doi:

459 10.1002/2014JE004732
460
461 Savijärvi H, Harri AM, Kemppinen O, 2016. The diurnal water cycle at Curiosity: role of exchange
462 with the regolith**.** Icarus 265, 63-69, doi:10.1016/j.icarus.2015.10.008
463
464 Seiff A, 1993. Mars atmospheric winds indicated by motion of the Viking landers during parachute
465 descent. J. Geophys. Res. 98, 7461-7474.
466
467 Seiff A, Kirk DB, 1977. Structure of the atmosphere of Mars in summer at mid-latitudes. J.
468 Geophys. Res. 82, 4364-4378.
469
470 Smith MD, 2004. Interannual variability in TES atmospheric observations of Mars during 1999-
471 2003. Icarus 167, 148-165.
472
473 Steele LJ, Balme MR, Lewis SR, Spiga A, 2017. The water cycle and regolith-atmosphere
474 interaction at Gale crater, Mars. Icarus 289, 56-79.
475
476 Zent AP, Hecht MH, Hudson TL, Wood SE, Chevrier VF, 2016. A revised calibration function and
477 results for the Phoenix mission TECP relative humidity sensor. J. Geophys. Res. (Planets) 121, 626-
478 651.

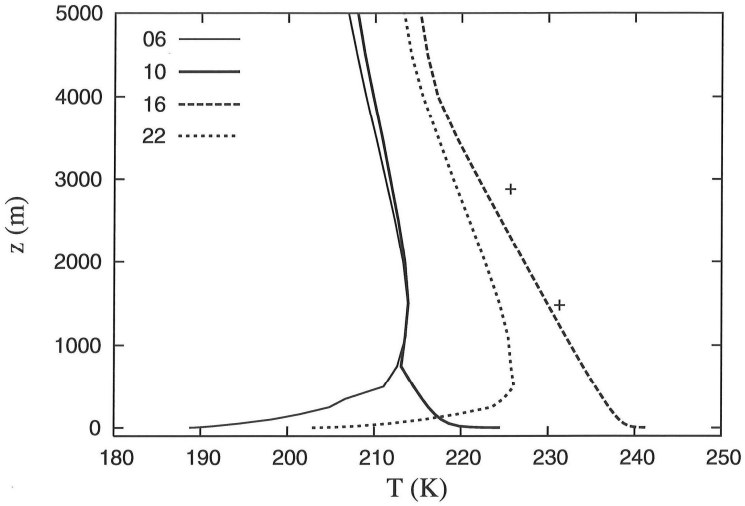


Figure 1. Temperature profiles from 1.6 m to 5000 m at 0600, 1000, 1600 and 2200LT from the VL-1 simulation. Also shown are two observed values at about 1615LT during the landing of VL-1.

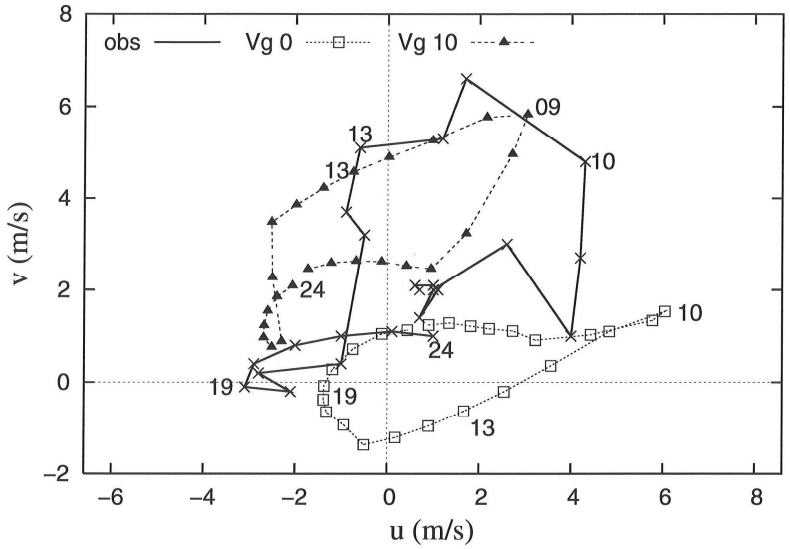


Figure 2. Mean diurnal wind hodograph for the first 44 sols of VL-1 (Hess et al., 1977, solid) with 1.6 m wind hodographs from the VL-1 simulation for no prevailing flow (V_g 0, squares), and for V_g of 10 m/s from south (triangles). Upslope of 0.1° is to WSW in the 1-D model.

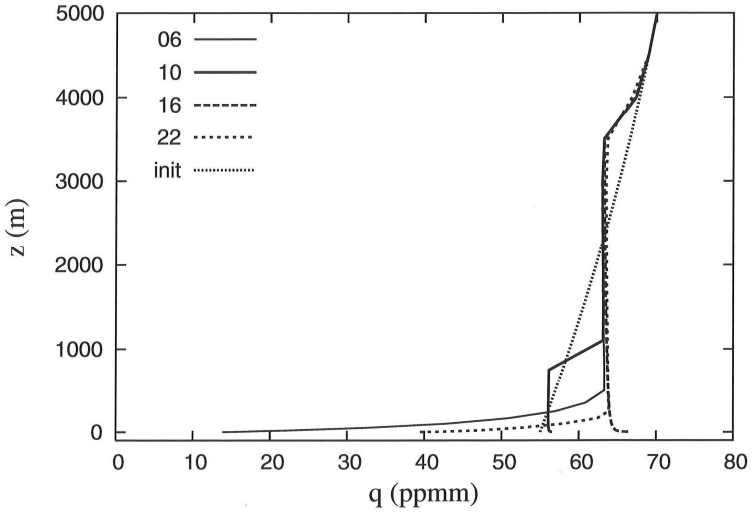


Figure 3. Water vapor mixing ratio profiles from 1.6 m to 5000 m initially (dots) and at 0600, 1000, 1600 and 2200LT in the VL-1 simulation with adsorption. PWC is 12.5 μm.

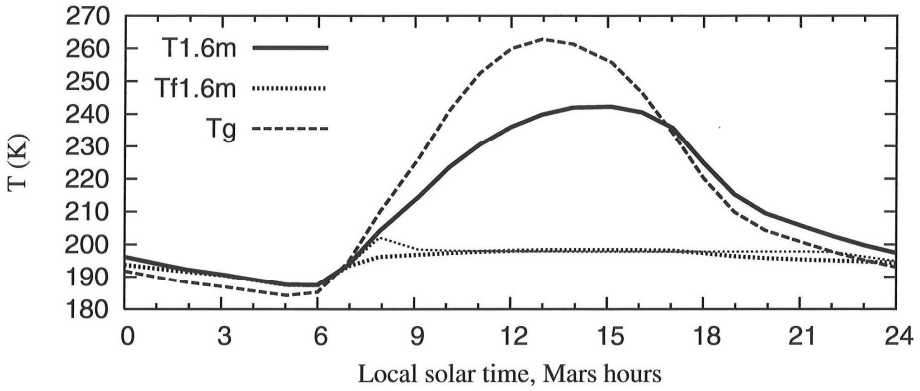


Figure 4. Hourly values of T at 1.6 m (solid line), the frost point temperature T_f at 1.6 m (dotted lines) and the surface temperature T_g (dashed line) in the VL-1 simulation with adsorption (thicker lines) and without adsorption (thinner lines).

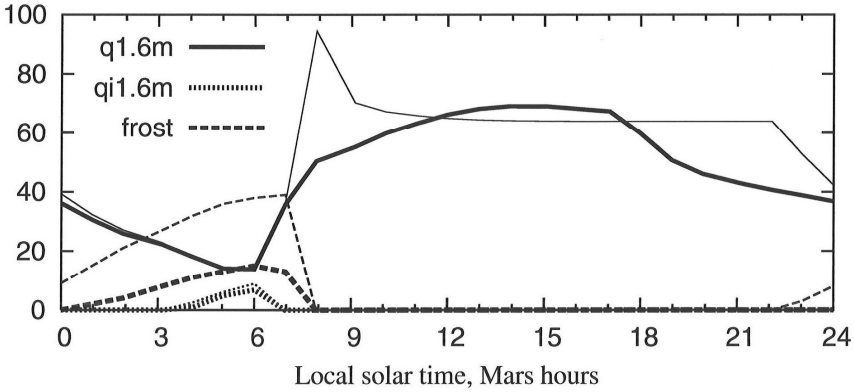


Figure 5. Hourly values of q at 1.6 m (solid lines, ppmm), q_i (i.e. fog) at 1.6 m (dotted lines, ppmm) and frost depth (dashed lines, 10^{-2} μm) in the VL-1 simulation with adsorption (thicker lines) and without adsorption (thinner lines).

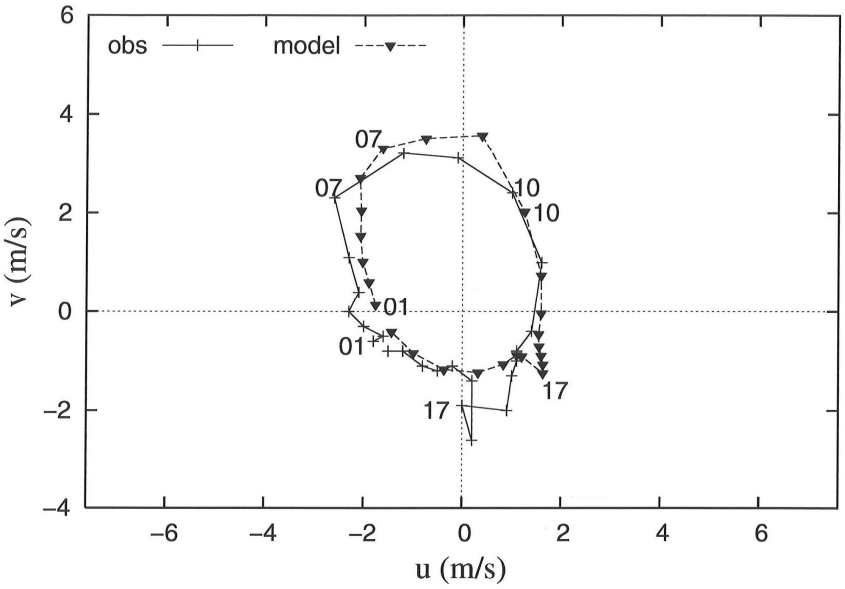


Figure 6. Mean diurnal wind hodograph for the first 50 sols of VL-2 (Hess et al., 1977, solid) and 1.6 m wind hodographs from the VL-2 simulation without prevailing flow (V_g 0, triangles).

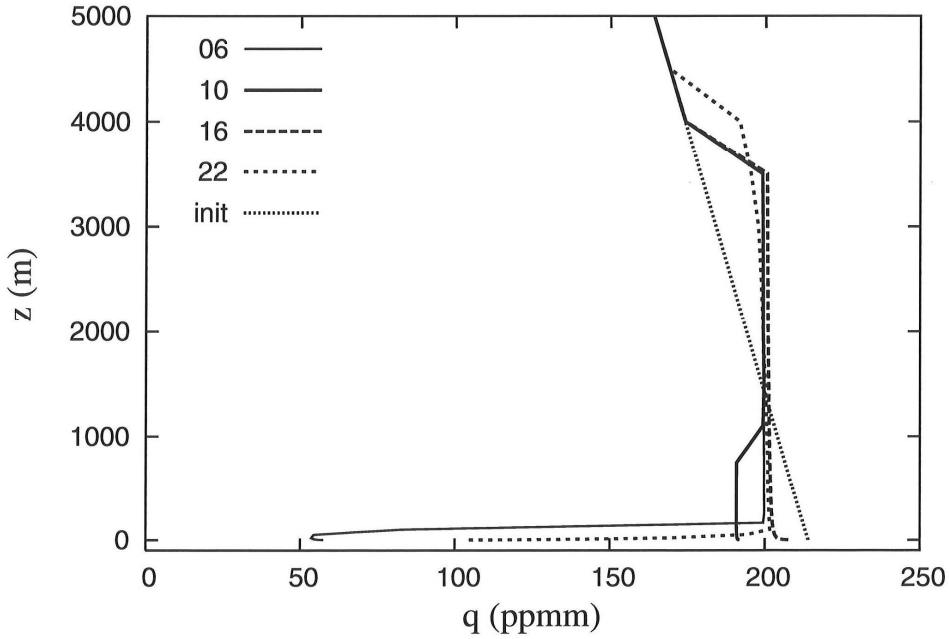


Figure 7. Water vapor mixing ratio profiles from 1.6 m to 5000 m initially (dots) and at 0600, 1000, 1600 and 2200LT in the VL-2 simulation with adsorption. PWC is 25 μm.

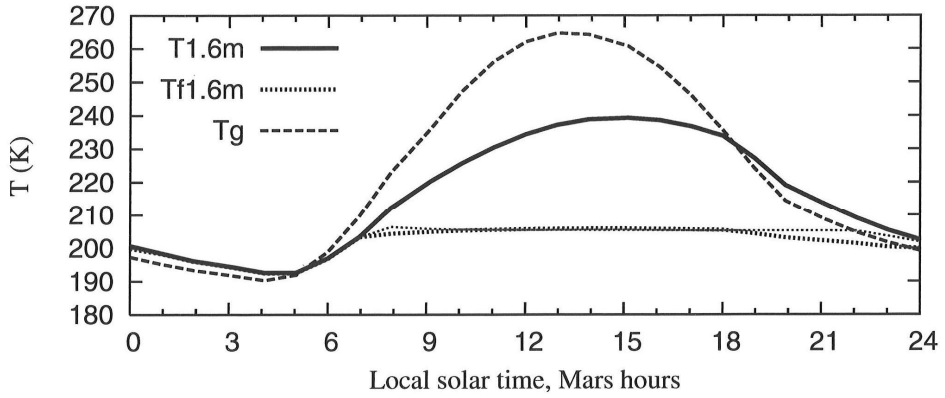


Figure 8. As Figure 4 but for VL-2.

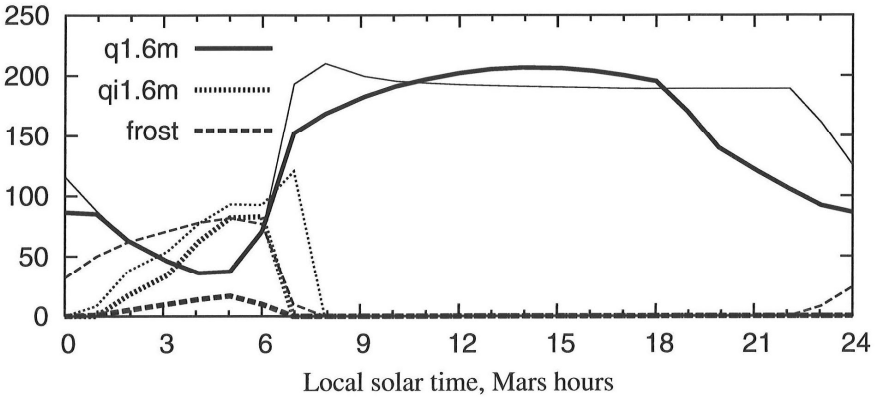


Figure 9. As Figure 5 but for VL-2.

4. Moisture results at VL-1

Moisture was not directly observed by the VL's but the column precipitable water content (PWC) was charted by MAWD onboard the orbiters. The vertical structure was, however, not constrained. Hence the initial profile of q (dots in Figure 6) is adopted from MCD for the VL-1 site at Ls 100^o (MCD PWC ~14 μm) and scaled to produce the MAWD-observed PWC of about 12.5 μm above VL-1 (J97, their fig. 1). The maximum of q is at about 10 km height, indicating the water pulse transported to the south from the sublimating northern icecap (Read and Lewis, 2004; Smith, 2004). Figure 6 displays the resulting diurnal (sol 3) q-profiles in the simulation with adsorption Strong convection mixes the water vapor evenly to about 65 ppmm in the lowest 4 km during every day. The vapor then stays well-mixed over the night except close to the surface, where it is strongly depleted in a shallow layer during the evening and night. The depleted moisture returns to the growing convective layer every morning (note the 1000LT curve) and hence PWC stays at around 12.5 μm from sol to sol in the integration (as observed by MAWD), provided porosity is set to 22% (35-40% was suggested for the MSL landing site and Rocknest in Savijärvi et al., 2016). There is only little diurnal variation in PWC because the depleted layer is so shallow by Figure 6.

Some validation for the near-surface values of q may be obtained from the fact that there possibly was a thin icefog during the night hours. Ryan and Sharman (1981) report inflections in the observed VL-1 temperatures during many nights and Pollack et al. (1977) display small night increases of 0-0.05 in optical depths for Ls 100-110^o. The temperature inflection was suggested to be due to the radiative effect of a developing fog. One typical example occurred on sol 21 at 0200-0300LT at T1.6m of 191K. Assuming p of 760 Pa, the respective ice-saturated value $q_{sat}(T,p)$ is 20.5 ppmm. This is between the model's 1.6 m q-values at 2200LT (40 ppmm) and 0600LT (14 ppmm) of Figure 6. Hence the numerical values of q appear realistic.

Figure 2 displayed frost point temperatures at 1.6 m (T_f) from the VL-1 simulation with adsorption (thick dots) and without adsorption (thin dots). We discuss first the simulation with adsorption. Its T_f hits T_g after 2300LT (frost then starting to form onto the cold ground), and T between 0200-0300LT (fog forming at 1.6 m) with a trace of an inflection in T at 191K as observed, although the inflection is weaker than in the observations. Figure 7 shows the respective mixing ratios of water vapor and water ice at 1.6 m (q, q_i in ppmm), and the frost depth (in 0.01 μm). In the adsorption simulation q (thick line) begins to decay rapidly after 1700LT because adsorption to ground is activated by the rapid decrease of T_g (Figure 2). This depletes humidity from the near-surface air as replenishment from the moister layers aloft (Figure 6) is inhibited by the weak turbulent mixing of the now stable surface layer. From 0000LT onward frost (thick dashed line) covers the ground, replacing adsorption as the moisture-depleting process. The thin layer of frost grows to mere 0.15 μm by sunrise and sublimates rapidly thereafter (the VL-1 cameras did not report any frost). At 0300LT icefog (thick dotted line) appears at 1.6 m, in accordance with the Ryan and Sharman suggestion. Fog grows to about 20 m height by 0600LT with q_i about 7 ppmm throughout. Its precipitable ice content is only 0.006 μm; too little to cause strong radiative warming though the optical depth of the atmosphere is slightly enhanced. Soon after sunrise (0530LT) fog sublimates back to vapor; then desorption and upward diffusion from the rapidly warming regolith releases more vapor, which mixes evenly to the growing convective boundary layer, as seen in Figure 6.

In the no-adsorption case q (thin line in Figure 7) stays nearly constant during the afternoon and evening until at about 2200LT the associated high T_f (thin dotted line in Figure 2) hits T_g and frost begins to strongly deposit onto the cold ground, consuming moisture from the air. At about 0230 fog (thin dotted line in Figure 7) does appear much as in the basic simulation. The thick frost layer grows here to a depth of 0.4 μm by 0700LT. It then sublimates rapidly back to vapor by 0800LT,

increasing q temporarily at 0800LT; such a morning peak in moisture was noted at Phoenix after frosty nights (Zent et al., 2016). After the peak q stays nearly constant late to the evening.

Because the fog and the temperatures are nearly similar in our simulation with and without adsorption, the VL-1 fog-related observations do not ascertain adsorption. On the other hand night frosts, which were strong in the model without adsorption, are not reported at VL-1 (Martinez et al., 2017). Moreover, VL-1 landed onto loose regolith: the three legs of the lander were buried several cm deep into it (Paton et al., 2016). Hence we believe that adsorption to porous regolith is likely at the VL-1 site.

We made some sensitivity tests about the robustness of the assumed values of PWC and porosity. Fedorova et al. (2010) have suggested lower values for retrieved PWC from MAWD, by about 40% for 22ºN at around Ls 100º. Hence the VL-1 simulations were repeated with the initial PWC scaled down to 7.5 μm. In this drier atmosphere no fog resulted. On the other hand PWC initially larger than 15 μm produced an early and thick fog.

The porosity of 22% was chosen here, because it conserved PWC from sol to sol (as observed). With PWC initially 12.5 μm, porosity of 40% led to a slow daily increase of PWC (to 13.5 μm by sol 4) and to a morning fog, which was increasingly too early and too thick, compared to the observations. Porosity of 10% produced on the other hand a slow reduction in PWC (to 12.2 μm by sol 4) and a fog, which was increasingly late and too thin. Admittedly, the value of 22% might be sensitive to the adsorption scheme chosen; we used here the J97 adsorption isotherm, which appeared the best for MSL REMS data in Savijärvi et al. (2016) and Steele et al. (2017). Other adsorption schemes were not tested.

5. Moisture results for VL-2

The near-surface midsummer air is relatively moist at the high-latitude VL-2 site, the polar water ice cap having sublimated completely. The MCD-based linearly upward decaying initial q(z) is scaled to PWC of 25 μm, as observed by MAWD above the VL-2 site at around L_s 120º (J97, their fig. 2; the MCD PWC is ~33 μm). Figure 8 shows the diurnal profiles of q in the VL-2 simulation with adsorption. The diurnal patterns resemble those at VL-1 (Figure 6) but the values are naturally higher at VL-2 because of the moist air. There is a well-mixed layer (q~200 ppmm) to about 4 km height in Figure 8, with strong depletion of q very near the surface during the evening and night. At 0600LT an increase in q can be seen just above the sun-warmed surface: sunrise occurred here at 0425LT, sublimating the night frost. Convection starts at about 0530LT when T_g exceeds T (Figure 4); stabilization ($T_g < T$) respectively at about 1800LT. The convective layer has grown to about 750 m by 1000LT in Figure 8.

Figure 9 shows the hourly moisture variables. Afternoon values of q are near 200 ppmm. Adsorption reduces q strongly after stabilization (thick line). Hence the frost point (thick dots in Figure 4) decreases rapidly in the evening, meeting T_g after 0000LT, when weak frost begins to deposit onto the ground. The very thin layer grows to 0.18 μm by 0500LT and disappears by 0700LT. Fog appears at 1.6 m at around 0100LT, reaching 111 ppmm by 0600LT with precipitable ice content of about 0.32 μm across the about 120 m high fog layer. It dissolves by 0800LT. The optical depth increases in the model accordingly from 0.30 at daytime (dust) to 0.42 by 0600LT (dust plus fog with particle-r_e of 5 μm assumed), as typically observed at VL-2 by imaging the sun about one hour before and after sunrise (Pollack et al., 1977; their figs. 2-3). The relatively high T_g and the strong evening depletion of water vapor by adsorption keep the frost amount low, despite high values of moisture of the early afternoon. The latter are partly due to desorption of water from

643 the rapidly warming regolith at 0700-1300LT, after frost has sublimated away by 0700LT. As
644 enthalpy of sublimation (46.7 kJ/mol) is higher compared to that of adsorption of water (about 23
645 kJ/mol according to REMS data, Savijärvi et al., 2015, 2016), the q-slopes are accordingly much
646 steeper in Figure 7 during the deposition (0100-0500LT) and sublimation (0500-0700LT) of frost
647 than during the periods of adsorption (1800-0100LT) and desorption (0700-1300LT).
648
649 In the VL-2 simulations without adsorption (porosity 0; thin lines in Figures 4, 9) q stays high until
650 about 2100LT, when T_g hits T_f and relatively strong formation of ground frost begins to rapidly
651 deplete air moisture. The frost depth grows here to 0.9 μm by 0500LT. Thick fog nevertheless
652 appears just after midnight. It reaches 161 ppmm at 1.6 m by 0700LT with optical depth up to 0.53.
653 Nearly the same is obtained by setting adsorption to 0 with non-scaled molecular/Knudsen diffusion
654 of water vapor active in the 22% porous regolith (see Savijärvi et al., 2016). Hence molecular
655 diffusion as such (i.e., without adsorption) appears to be ineffective in the diurnal-scale water vapor
656 exchange in the top regolith.
657
658 Ryan and Sharman (1981, their Table 1) report for sols 1-15 of VL-2 a composite 1.6 m temperature
659 inflection at around 0130LT (199K), with fog formation suggested as the reason. Our adsorption
660 simulation agrees nicely with this, but the two no-adsorption simulations induce fog too early
661 (0000LT vs. 0130LT) and the nocturnal increase in optical depth is too large in them (0.23 vs. the
662 observed 0.1-0.15). Furthermore, the inflection-based estimate for PWC is 10.5-12 μm for VL-2 at
663 around L_s 120^o in J97 (their fig. 2). A similar estimate from the adsorption simulation (i.e. having
664 the 0130LT q at 1.6 m vertically constant in the q-integration for PWC) produces 11 μm, but from
665 the no-adsorption simulations, 15 μm. It thus appears that adsorption is very likely at the VL-2 site
666 in summer.
667
668 In the mesoscale simulations of Steele et al. (2017) night frosts appear in the surrounding regions of
669 the Gale crater. During the moist season (Ls 180^o) they amount to depths of ~0.2-0.3 μm with
670 adsorption and to ~0.8 μm without adsorption, rather similarly with the above VL-2 results.
671 When the VL-2 simulation was repeated with the initial PWC scaled to 15 μm (40% lower), fog
672 appeared between 0300-0400LT, i.e. too late; and there was no increase in optical depth. As MCD
673 PWC was about 34 μm and the MY26-34 retrievals of PWC for the latitude and season are in the
674 22-35 μm range by TES and CRISM, we believe that the MAWD PWC of 25 μm is realistic.
675
676 The porosity of 22% conserved PWC from sol to sol also in the VL-2 simulation. With PWC
677 initially 25 μm, porosity of 40% led to a slow increase of PWC (to 27.5 μm by sol 4) and to a
678 morning fog, which was increasingly too early and too thick, while porosity of 10% produced slow
679 reduction in PWC and a fog, which was increasingly late and too thin.
680
681